ACS Medicinal Chemistry Letters



pubs.acs.org/acsmedchemlett
Letter

# Beyond Neddylation Inhibition: X-ray Structures Reveal Carbonic Anhydrase Isoform Selectivity of Pevonedistat

Chiara Baroni, Marta Ferraroni, Claudiu T. Supuran, and Andrea Angeli*

Cite This: ACS Med. Chem. Lett. 2026, 17, 1393−1397



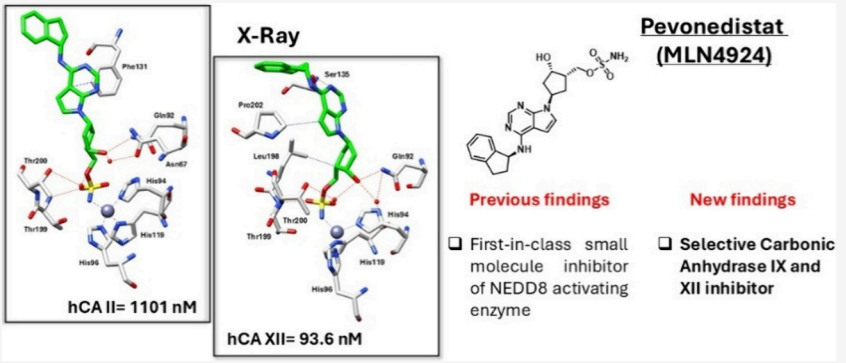


**ABSTRACT:** Pevonedistat (MLN4924) is a first-in-class inhibitor of the NEDD8-activating enzyme that blocks protein neddylation and exhibits antitumor activity in multiple clinical phases. Here, we report a previously unrecognized and isoform-selective inhibitory profile of pevonedistat against the tumor-associated isoforms human carbonic anhydrase IX and XII (hCA IX and XII). To elucidate the structural basis of this selectivity, X-ray crystal structures were determined for pevonedistat in complex with hCA I, hCA II, and an engineered hCA II variant mimicking hCA XII. These findings provide a mechanistic explanation for the known preferential partitioning of pevonedistat into whole blood via binding to erythrocyte CAs and suggest that CA inhibition may contribute to its antitumor activity in hypoxic tumor microenvironments where hCA IX and XII are overexpressed. This study reveals a dual functional profile for pevonedistat, linking neddylation inhibition with selective targeting of tumor-associated CAs and offers to exploit this synergy in anticancer drug design.

**KEYWORDS:** *carbonic anhydrase, metalloenzyme, pevonedistat, tumor, neddylation, sulfamate*



Pevonedistat (also known as MLN4924 or TAK-924) is an adenosine sulfamate analog and the first-in-class small molecule inhibitor of the neural precursor cell expressed developmentally downregulated 8 (NEDD8) activating enzyme (NAE) (Figure 1).[1] It acts by forming a covalent adduct that mimics the adenylated NEDD8 intermediate, thereby preventing formation of the thioester bond required for downstream transfer steps in the neddylation cascade.[1,2]

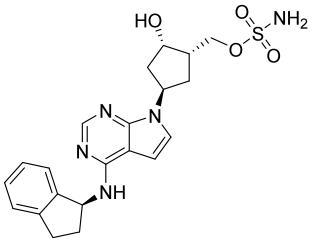

**Figure 1.** Structure of pevonedistat (MLN4924).

This conjugation pathway, termed neddylation, is mechanistically and structurally analogous to ubiquitination. Indeed, NEDD8 shares significant sequence homology with ubiquitin and functions via a similar mechanism.[1,3,4] The E1 enzyme responsible for NEDD8 activation, NEDD8-activating enzyme E1 regulatory subunit, forms a heterodimer with Ubiquitin-like modifier-activating enzyme 3 (UBA3). This complex catalyzes ATP-dependent adenylation of NEDD8 to form a NEDD8-AMP intermediate within the nucleotide-binding pocket, followed by transfer to a catalytic cysteine residue to generate a thioester-linked NEDD8−NAE intermediate. Binding of a second NEDD8-AMP molecule induces a conformational state that promotes transfer of the first NEDD8 to the cognate E2

Received: April 9, 2026
Revised: May 3, 2026
Accepted: May 15, 2026
Published: May 27, 2026





https://doi.org/10.1021/acsmedchemlett.6c00197
ACS Med. Chem. Lett. 2026, 17, 1393−1397

conjugating enzyme.[1] Approximately 20% of cellular proteins are degraded through the ubiquitin-proteasome system (UPS), largely regulated by Cullin-RING ubiquitin ligase (CRL) E3 ligases. Activation of cullins requires covalent conjugation of NEDD8, making neddylation a critical regulatory step for CRL activity.[5] Dysregulation of this pathway has been implicated in multiple pathophysiological processes, including cell survival and differentiation, neurodegeneration, and cancer.[6−8] Dysregulation of neddylation signaling in cancer is well documented, with multiple studies reporting overexpression of NEDD8 and its associated enzymes in tumor tissues.[5] By inactivating CRL, pevonedistat exhibits pronounced antitumor activity and have advanced through numerous Phase I/II clinical trials for the treatment of both hematological malignancies and solid tumors.[1,9] It has also been evaluated in Phase III clinical trials in combination with azacitidine for the treatment of Acute Myeloid Leukemia.[10−13] An important pharmacokinetic observation emerging from these studies is the substantially higher concentration of pevonedistat in whole blood compared with plasma.[14] This preferential partitioning into red blood cells has been attributed to binding to ubiquitous human carbonic anhydrases (CAs, EC 4.2.1.1) I and II, two highly abundant isoforms present in erythrocytes.[15] CAs are zinc metalloenzymes that catalyze the reversible hydration of carbon dioxide to bicarbonate and a proton.[16,17] The binding of pevonedistat to these enzymes provides a plausible explanation for the extensive whole-blood distribution observed in both animal models and humans.[14] On the other hand, in solid tumors, hypoxic conditions and the resulting acidic microenvironment confer a selective advantage to malignant cells.[18] To survive under acidic and hypoxic stress, tumor cells upregulate mechanisms that maintain intracellular pH within a slightly alkaline range conducive to proliferation and survival.[19,20] Among these adaptations is the overexpression of the tumor-associated isoforms hCA IX and XII.[17,20] Consequently, increasing evidence supports CA inhibition as a promising anticancer strategy.[21−23] In this context, the presence of a sulfamate moiety in the pevonedistat scaffold may contribute to its antitumor activity. In fact, the sulfamate is a recognized bioisostere of the sulfonamide, the typical zinc binding group of CAs, and is itself a characteristic zinc-binding motif in CA inhibitors. This dual functionality provides a mechanistic rationale for a synergistic effect arising from the combination of neddylation inhibition and CA inhibition in solid tumors. The inhibitory activity of pevonedistat was evaluated against all catalytically active human CA isoforms (hCA I-XIV) and compared with the reference inhibitor acetazolamide (AAZ) and the clinically used sulfamate topiramate, using a stopped-flow $CO_2$ hydration assay (Table 1).

Cytosolic isoforms (hCA I, II, III, VII, and XIII) were inhibited by pevonedistat to varying degrees. Notably, hCA I displayed comparable inhibition to both topiramate and AAZ ($K_I$ = 262.6 nM), and none of the tested compounds inhibited hCA III. In contrast, pevonedistat exhibited markedly weaker inhibition against hCA II ($K_I$ = 1101 nM), approximately 3 orders of magnitude less potent than AAZ and topiramate. Among the remaining cytosolic isoforms, hCA VII was one of the most effectively inhibited with a $K_I$ of 75.8 nM, whereas hCA XIII showed moderate inhibition ($K_I$ = 323.8 nM), similar to that observed for hCA I. Regarding mitochondrial isoforms (hCA VA and VB), pevonedistat demonstrated weak inhibitory activity, with $K_I$ values in the high nanomolar to low micromolar range (709.1 nM and 2870 nM, respectively). In contrast, both AAZ and topiramate exhibited significantly stronger inhibition in the midnanomolar range. Similarly, hCA VI was inhibited by pevonedistat with a $K_I$ of 830 nM, corresponding to an approximately 18-fold and 75-fold reduction in potency compared to topiramate and AAZ, respectively. For the membrane-associated isoform hCA IV, pevonedistat displayed inhibition comparable to AAZ ($K_I$ = 93.7 vs 74.0 nM), whereas topiramate was over 50-fold less potent. Importantly, the tumor-associated isoforms hCA IX and XII were effectively inhibited by pevonedistat. In particular, hCA IX showed the strongest inhibition ($K_I$ = 59.1 nM), comparable to both AAZ and topiramate, while hCA XII was inhibited with moderate potency ($K_I$ = 93.6 nM). Finally, hCA XIV was weakly inhibited by pevonedistat ($K_I$ = 1959 nM), similarly to topiramate. Overall, pevonedistat demonstrates a favorable inhibition profile, with potent activity against tumor-associated isoforms (hCA IX and XII) comparable to AAZ and topiramate, while exhibiting reduced activity against off-target isoforms such as hCA I and II. This enhanced selectivity may contribute to its therapeutic efficacy in solid tumors, where these hCAs isoforms are overexpressed.[24−26]

**Table 1. Inhibition Data of All Catalytically Active Human CAs (hCA I−XIV) with Pevonedistat, Topiramate and AAZ Determined by a Stopped-Flow $CO_2$ Hydrase Assay**

| | $K_I$ (nM)[a] | | |
|---|---|---|---|
| Compd | Pevonedistat | AAZ | Topiramate |
| **hCA I** | 262.6 | 250.0 | 250.0 |
| **hCA II** | 1101 | 12.1 | 10.0 |
| **hCA III** | >10000 | >10000 | >10000 |
| **hCA IV** | 93.7 | 74.0 | 4900 |
| **hCA VA** | 709.1 | 63.0 | 63.0 |
| **hCA VB** | 2870 | 54.0 | 30.0 |
| **hCA VI** | 830.0 | 11.0 | 45.0 |
| **hCA VII** | 75.8 | 2.5 | 0.9 |
| **hCA IX** | 59.1 | 25.7 | 58.0 |
| **hCA XII** | 93.6 | 5.7 | 3.8 |
| **hCA XIII** | 323.8 | 17.0 | 47.0 |
| hCA XIV | 1959 | 41.0 | 1460 |

[a]Mean from 3 different assays, by a stopped flow technique (errors were in the range of ±5−10% of the reported values).

To rationalize the selectivity of pevonedistat toward tumor-associated CA isoforms, X-ray crystal structures were determined for hCA I, hCA II, and an engineered hCA II variant carrying active-site mutations designed to mimic hCA XII, (hCA XII mimic[27]) each in complex with pevonedistat. In all structures, the inhibitor displayed well-defined electron density within the active site (Figure S1), allowing unambiguous modeling of its binding mode. In every adduct, the sulfamate group coordinates the catalytic Zn ion in its deprotonated form,[28] in a manner analogous to classical sulfonamide inhibitors (Figure 2).[29] Consistently across the three complexes, one sulfamate oxygen forms a hydrogen bond with the backbone amide of Thr199, a conserved interaction known to stabilize inhibitors of this class within the CA active site (Figure 2).[28−31] In the hCA I complex, a single van der Waals interaction is observed between Leu198 and the pentacyclic core of the inhibitor (Figure 2A). The adenine moiety forms a hydrogen bond with Pro201 and participates in two water bridge interactions involving Gln92 and His200.


https://doi.org/10.1021/acsmedchemlett.6c00197
ACS Med. Chem. Lett. 2026, 17, 1393−1397

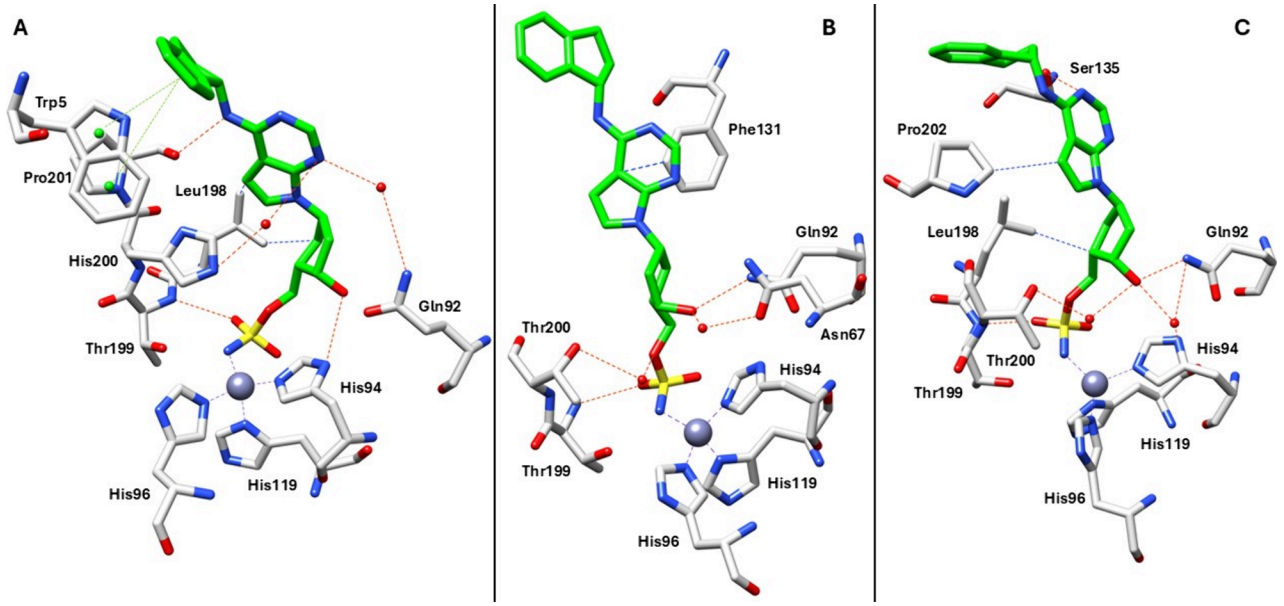


**Figure 2.** X-ray crystal structure of pevonedistat bound with hCA I (**A**, PDB: 29UD), hCA II (**B**, PDB: 29UH) and hCA XII mimic (**C**, PDB: 29UX). Residues involved in the binding of inhibitor are also shown; the gray sphere represents the zinc ion in the active site of the proteins. The purple dotted lines show the coordination of the zinc ion, van der Waals interactions are shown in blue, hydrogen bonds and water bridge are shown in red, $\pi$-stacking interactions are shown in green.

Additionally, the phenyl ring of the dihydro-indene tail engages in double $\pi$-stacking interactions with the aromatic side chain of Trp5, further stabilizing the inhibitor within the binding pocket (Figure 2A). In the hCA II complex, two water bridges are also present but involved different residues and portions of the inhibitor (Figure 2B). One water molecule bridges Thr200 and sulfamate oxygen, similarly to interactions reported for aliphatic sulfamides.[30,31] The second water bridge connects the alcohol group of the pentacyclic ring with Asn67; this hydroxyl group also forms a hydrogen bond with Gln92. Only a single van der Waals interaction is observed, between Phe131 and the adenine ring (Figure 2B). A comparison of the hCA I and hCA II complexes reveals a reduced number of favorable interactions in hCA II, consistent with the weaker inhibition observed for hCA II relative to hCA I ($K_I$ = 1101 nM vs 262.6 nM). Moving on the hCA XII mimic complex, two water bridge interactions again involve the alcohol group of the pentacyclic ring (Figure 2C). One water bridge connects this group with Gln92 and His94, while the second involves Thr200. This interaction network reorients the cyclopentyl portion of the inhibitor, restoring the van der Waals contact with Leu198 observed in hCA I but absent in hCA II. A key determinant is residue 131. In hCA II, Phe131 sterically constrains the inhibitor tail in a suboptimal orientation that limits contacts (Figure S2). In the hCA XII mimic, replacement of Phe131 with the less bulky Ala131 allows the tail to locate deeper into the hydrophobic pocket.

This repositioning enables a van der Waals interaction with Pro201 and a hydrogen bond between the adenine moiety and Ser135 (Figure 2C). This distinct position of pevonistat in the hCA XII mimic relative to hCA II provides a structural rationale for the higher inhibitory potency and selectivity of pevonedistat toward the tumor-associated isoform hCA XII. In summary, pevonedistat, classically recognized as first-in-class inhibitor of NAE, also displays a previously underappreciated and isoform selective inhibitory profile against CA isoforms. Kinetic analyses demonstrated preferential inhibition of the tumor-associated isoforms hCA IX and XII. X-ray crystallographic studies provided a structural rationale for this selectivity, revealing how active-site residue differences modulate the positioning of the inhibitor and govern productive hydrophobic, $\pi$-stacking, and water bridge interactions. These findings not only explain the extensive whole-blood partitioning of pevonedistat through interaction with erythrocyte CAs but also suggest that CA inhibition may contribute to its antitumor activity in hypoxic tumors where hCA IX and XII are overexpressed. Collectively, our study reveals a dual mechanistic dimension for pevonedistat, linking neddylation inhibition with selective targeting of tumor-associated CAs, and provides a structural framework for exploiting this synergy in anticancer drug design.

## ■ ASSOCIATED CONTENT

### Supporting Information

The Supporting Information is available free of charge at https://pubs.acs.org/doi/10.1021/acsmedchemlett.6c00197.

Experimental sections, supplementary figures and X-ray data collections (PDF)

## ■ AUTHOR INFORMATION


### Corresponding Author

**Andrea Angeli** − *NEUROFARBA Department, Sezione di Scienze Farmaceutiche, University of Florence, 50019 Florence, Italy;* orcid.org/0000-0002-1470-7192; Email: andrea.angeli@unifi.it

### Authors

**Chiara Baroni** − *Department of Chemistry "Ugo Schiff", University of Florence, I-50019 Florence, Italy*

**Marta Ferraroni** − *Department of Chemistry "Ugo Schiff", University of Florence, I-50019 Florence, Italy;* orcid.org/0000-0001-7258-738X




https://doi.org/10.1021/acsmedchemlett.6c00197
ACS Med. Chem. Lett. 2026, 17, 1393−1397

**Claudiu T. Supuran** − *NEUROFARBA Department, Sezione di Scienze Farmaceutiche, University of Florence, 50019 Florence, Italy;* orcid.org/0000-0003-4262-0323

Complete contact information is available at: https://pubs.acs.org/10.1021/acsmedchemlett.6c00197

### Author Contributions

All authors have given approval to the final version of the manuscript.

### Notes

No unexpected or unusually high safety hazards were encountered.

The authors declare no competing financial interest.

## ■ ACKNOWLEDGMENTS

We gratefully acknowledge Elettra and XRD2 beamline for providing beamtime and support under proposal mx20220596 and we would like to thank Nicola Demitri for assistance and support in using the beamline.

## ■ ABBREVIATIONS

NEDD8, neural precursor cell expressed developmentally downregulated 8; NAE NEDD8, activating enzyme; UBA3, Ubiquitin-like modifier-activating enzyme 3; UPS, ubiquitin-proteasome system; CRL, Cullin-RING ubiquitin ligase; CA, Carbonic Anhydrase; CAI, Carbonic Anhydrase Inhibitors; AAZ, acetazolamide

## ■ REFERENCES

(1) Soucy, T. A.; Smith, P. G.; Milhollen, M. A.; Berger, A. J.; Gavin, J. M.; Adhikari, S.; Brownell, J. E.; Burke, K. E.; Cardin, D. P.; Critchley, S.; Cullis, C. A.; Doucette, A.; Garnsey, J. J.; Gaulin, J. L.; Gershman, R. E.; Lublinsky, A. R.; McDonald, A.; Mizutani, H.; Narayanan, U.; Olhava, E. J.; Peluso, S.; Rezaei, M.; Sintchak, M. D.; Talreja, T.; Thomas, M. P.; Traore, T.; Vyskocil, S.; Weatherhead, G. S.; Yu, J.; Zhang, J.; Dick, L. R.; Claiborne, C. F.; Rolfe, M.; Bolen, J. B.; Langston, S. P. An inhibitor of NEDD8-activating enzyme as a new approach to treat cancer. *Nature.* **2009**, *458*, 732−736.

(2) Mohan, S. P.; NareshKumar, R. N.; Cheruvu, S. S.; Nagarajan, H.; Majid, N. F.; Ranganathan, S.; Nirmal, J.; Ramasubramanyan, S. MLN4924, neddylation inhibitor suppresses hypoxia induced retinal angiogenesis by targeting Human Antigen R signaling. *Life Sci.* **2025**, *380*, 123927.

(3) Enchev, R. I.; Schulman, B. A.; Peter, M. Protein neddylation: beyond cullin-RING ligases. *Nat. Rev. Mol. Cell Biol.* **2015**, *16*, 30−44.

(4) Zhou, L.; Jiang, Y.; Luo, Q.; Li, L.; Jia, L. Neddylation: a novel modulator of the tumor microenvironment. *Mol. Cancer.* **2019**, *18*, 77.

(5) Zubiete-Franco, I.; Fernández-Tussy, P.; Barbier-Torres, L.; Simon, J.; Fernández-Ramos, D.; Lopitz-Otsoa, F.; Gutiérrez-de Juan, V.; de Davalillo, S. L.; Duce, A. M.; Iruzubieta, P.; Taibo, D.; Crespo, J.; Caballeria, J.; Villa, E.; Aurrekoetxea, I.; Aspichueta, P.; Varela-Rey, M.; Lu, S. C.; Mato, J. M.; Beraza, N.; Delgado, T. C.; Martínez-Chantar, M. L. Deregulated neddylation in liver fibrosis. *Hepatology.* **2017**, *65*, 694−709.

(6) Zhou, X.; Tan, M.; Nyati, M. K.; Zhao, Y.; Wang, G.; Sun, Y. Blockage of neddylation modification stimulates tumor sphere formation in vitro and stem cell differentiation and wound healing in vivo. *Proc. Natl. Acad. Sci. U. S. A.* **2016**, *113*, No. E2935.

(7) Vogl, A. M.; Brockmann, M. M.; Giusti, S. A.; Maccarrone, G.; Vercelli, C. A.; Bauder, C. A.; Richter, J. S.; Roselli, F.; Hafner, A. S.; Dedic, N.; Wotjak, C. T.; Vogt-Weisenhorn, D. M.; Choquet, D.; Turck, C. W.; Stein, V.; Deussing, J. M.; Refojo, D. Neddylation inhibition impairs spine development, destabilizes synapses and deteriorates cognition. *Nat. Neurosci.* **2015**, *18*, 239−251.

(8) Kuo, K. L.; Ho, I. L.; Shi, C. S.; Wu, J. T.; Lin, W. C.; Tsai, Y. C.; Chang, H. C.; Chou, C. T.; Hsu, C. H.; Hsieh, J. T.; Chang, S. C.; Pu, Y. S.; Huang, K. H. MLN4924, a novel protein neddylation inhibitor, suppresses proliferation and migration of human urothelial carcinoma: In vitro and in vivo studies. *Cancer Lett.* **2015**, *363*, 127−136.

(9) Swords, R. T.; Coutre, S.; Maris, M. B.; Zeidner, J. F.; Foran, J. M.; Cruz, J.; Erba, H. P.; Berdeja, J. G.; Tam, W.; Vardhanabhuti, S.; Pawlikowska-Dobler, I.; Faessel, H. M.; Dash, A. B.; Sedarati, F.; Dezube, B. J.; Faller, D. V.; Savona, M. R. Pevonedistat, a first-in-class NEDD8-activating enzyme inhibitor, combined with azacitidine in patients with AML. *Blood.* **2018**, *131*, 1415−1424.

(10) Adès, L.; Girshova, L.; Doronin, V. A.; Díez-Campelo, M.; Valcárcel, D.; Kambhampati, S.; Viniou, N. A.; Woszczyk, D.; De Paz Arias, R.; Symeonidis, A.; Anagnostopoulos, A.; Munhoz, E. C.; Platzbecker, U.; Santini, V.; Fram, R. J.; Yuan, Y.; Friedlander, S.; Faller, D. V.; Sekeres, M. A. Pevonedistat plus azacitidine vs azacitidine alone in higher-risk MDS/chronic myelomonocytic leukemia or low-blast-percentage AML. *Blood Adv.* **2022**, *6*, 5132−5145.

(11) Swords, R. T.; Coutre, S.; Maris, M. B.; Zeidner, J. F.; Foran, J. M.; Cruz, J.; Erba, H. P.; Berdeja, J. G.; Tam, W.; Vardhanabhuti, S.; Pawlikowska-Dobler, I.; Faessel, H. M.; Dash, A. B.; Sedarati, F.; Dezube, B. J.; Faller, D. V.; Savona, M. R. Pevonedistat, a first-in-class NEDD8-activating enzyme inhibitor, combined with azacitidine in patients with AML. *Blood.* **2018**, *131*, 1415−1424.

(12) Qin, A.; Wells, L.; Malhotra, B.; Gadgeel, S.; Schneider, B. J.; Ramnath, N.; Rice, J. D.; Kalemkerian, G. P. A Phase II Trial of Pevonedistat and Docetaxel in Patients With Previously Treated Advanced Non-Small-Cell Lung Cancer. *Clin Lung Cancer.* **2024**, *25*, 128−134.

(13) Foster, J. H.; Reid, J. M.; Minard, C.; Woodfield, S.; Denic, K. Z.; Isikwei, E.; Voss, S. D.; Nelson, M.; Liu, X.; Berg, S. L.; Fox, E.; Weigel, B. J. Phase 1 study of NEDD8 activating enzyme inhibitor pevonedistat in combination with chemotherapy in pediatric patients with recurrent or refractory solid tumors (ADVL1615). *Eur. J. Cancer.* **2024**, *209*, 114241.

(14) Zhou, X.; Sedarati, F.; Faller, D. V.; Zhao, D.; Faessel, H. M.; Chowdhury, S.; Bolleddula, J.; Li, Y.; Venkatakrishnan, K.; Papai, Z. Phase I study assessing the mass balance, pharmacokinetics, and excretion of [$^{14}$C]-pevonedistat, a NEDD8-activating enzyme inhibitor in patients with advanced solid tumors. *Invest New Drugs.* **2021**, *39*, 488−498.

(15) Aliakbar, S.; Brown, P. R. Measurement of human erythrocyte CAI and CAII in adult, newborn, and fetal blood. *Clin Biochem.* **1996**, *29*, 157−164.

(16) D'Ambrosio, K.; Di Fiore, A.; Alterio, V.; Langella, E.; Monti, S. M.; Supuran, C. T.; De Simone, G. Multiple Binding Modes of Inhibitors to Human Carbonic Anhydrases: An Update on the Design of Isoform-Specific Modulators of Activity. *Chem. Rev.* **2025**, *125*, 150−222.

(17) Supuran, C. T. Carbonic anhydrases: novel therapeutic applications for inhibitors and activators. *Nat. Rev. Drug Discovery* **2008**, *7*, 168−181.

(18) Petrova, V.; Annicchiarico-Petruzzelli, M.; Melino, G.; Amelio, I. The hypoxic tumour microenvironment. *Oncogenesis.* **2018**, *7*, 10.

(19) Angeli, A.; Carta, F.; Nocentini, A.; Winum, J. Y.; Zalubovskis, R.; Akdemir, A.; Onnis, V.; Eldehna, W. M.; Capasso, C.; Simone, G.; Monti, S. M.; Carradori, S.; Donald, W. A.; Dedhar, S.; Supuran, C. T. Carbonic Anhydrase Inhibitors Targeting Metabolism and Tumor Microenvironment. *Metabolites.* **2020**, *10*, 412.

(20) Neri, D.; Supuran, C. T. Interfering with pH regulation in tumours as a therapeutic strategy. *Nat. Rev. Drug Discovery* **2011**, *10*, 767−777.

(21) Ronca, R.; Supuran, C. T. Carbonic anhydrase IX: An atypical target for innovative therapies in cancer. *Biochim Biophys Acta Rev. Cancer.* **2024**, *1879*, 189120.

(22) Kalinin, S.; Malkova, A.; Sharonova, T.; Sharoyko, V.; Bunev, A.; Supuran, C. T.; Krasavin, M. Carbonic Anhydrase IX Inhibitors as

Candidates for Combination Therapy of Solid Tumors. *Int. J. Mol. Sci.* **2021**, *22*, 13405.
(23) Supuran, C. T. Carbonic Anhydrase Inhibition and the Management of Hypoxic Tumors. *Metabolites.* **2017**, *7*, 48.
(24) Shoji, H.; Takahari, D.; Ooki, A.; Hirano, H.; Okita, N.; Nagashima, K.; Adachi, J.; Yamaguchi, K.; Kato, K.; Boku, N. Phase I study of pevonedistat combined with capecitabine and oxaliplatin in patients with platinum-refractory advanced gastric cancer. *Sci. Rep.* **2026**, *16*, 692.
(25) Tang, H.; Pang, X.; Li, S.; Tang, L. The Double-Edged Effects of MLN4924: Rethinking Anti-Cancer Drugs Targeting the Neddylation Pathway. *Biomolecules.* **2024**, *14*, 738.
(26) Foster, J. H.; Reid, J. M.; Minard, C.; Woodfield, S.; Denic, K. Z.; Isikwei, E.; Voss, S. D.; Nelson, M.; Liu, X.; Berg, S. L.; Fox, E.; Weigel, B. J. Phase 1 study of NEDD8 activating enzyme inhibitor pevonedistat in combination with chemotherapy in pediatric patients with recurrent or refractory solid tumors (ADVL1615). *Eur. J. Cancer.* **2024**, *209*, 114241.
(27) Genis, C.; Sippel, K. H.; Case, N.; Cao, W.; Avvaru, B. S.; Tartaglia, L. J.; Govindasamy, L.; Tu, C.; Agbandje-McKenna, M.; Silverman, D. N.; Rosser, C. J.; McKenna, R. Design of a carbonic anhydrase IX active-site mimic to screen inhibitors for possible anticancer properties. *Biochemistry.* **2009**, *48*, 1322−1331.
(28) Lopez, M.; Paul, B.; Hofmann, A.; Morizzi, J.; Wu, Q. K.; Charman, S. A.; Innocenti, A.; Vullo, D.; Supuran, C. T.; Poulsen, S. A. S-glycosyl primary sulfonamides-a new structural class for selective inhibition of cancer-associated carbonic anhydrases. *J. Med. Chem.* **2009**, *52*, 6421−6432.
(29) Langella, E.; Esposito, D.; Monti, S. M.; Supuran, C. T.; De Simone, G.; Alterio, V. A Combined in Silico and Structural Study Opens New Perspectives on Aliphatic Sulfonamides, a Still Poorly Investigated Class of CA Inhibitors. *Biology (Basel).* **2023**, *12*, 281.
(30) Angeli, A.; Ferraroni, M.; Nocentini, A.; Selleri, S.; Gratteri, P.; Supuran, C. T.; Carta, F. Polypharmacology of epacadostat: a potent and selective inhibitor of the tumor associated carbonic anhydrases IX and XII. *Chem. Commun. (Camb).* **2019**, *55*, 5720−5723.
(31) Angeli, A.; Ferraroni, M.; Supuran, C. T. Famotidine, an Antiulcer Agent, Strongly Inhibits Helicobacter pylori and Human Carbonic Anhydrases. *ACS Med. Chem. Lett.* **2018**, *9*, 1035−1038.


https://doi.org/10.1021/acsmedchemlett.6c00197
*ACS Med. Chem. Lett.* 2026, 17, 1393−1397